Aeronautical livery coating with icephobic property

L. Mazzola*

The main problem for the aircrafts is the ice formation on critical components (leading edges, slats, vertical tails, etc …) that decreases reliability and safety of the flights. The objectives of this work are mainly two. The former is to design and develop a new multifunctional coating with aesthetical (livery effect) and icephobic properties other than high adhesion and abrasion resistance. The latter is to design and realise a new tool to use with classical contact angle measurement techniques. This tool allows to replicate the same thermodynamic conditions (in terms of pressure and temperature) present at flight altitude. In fact it was demonstrated that the water contact angle changes, varying at the same time pressure and temperature. The experimental results corroborated the influence of temperature and pressure on the shape of the supercooled water droplet applied on the new icephobic coating. The high durability of the new anti-ice livery coating was determined thorough several mechanical tests such as cutting and tape test, pull-off tests and nanoindentation tests.

Keywords: Icephobic coating, Surface free energy, Wettability, Hierarchical structures, Unmanned air vehicle (UAV)

Introduction

The icing mitigation systems can be divided in anti-icing systems and de-icing systems. Amongst the anti-ice systems, the application of icephobic coatings is one of the possible methods for preventing the icing of aeronautical components (leading edges, wings, radomes, etc.).[1–8] Ice changes the laminar airflow, increasing drag while decreasing the ability of the airfoil to create lift. Ice accumulates on every exposed frontal surface of the airplane, not just on the wings, propeller and windshield, but also on the antennas, vents, intakes and cowlings.[9] The main function of icephobic coatings is to reduce the adhesive forces between the supercooled water or ice and the surface of the component. In particular, it is necessary to extend and to retain this ability during long-term operation.[10] The design of new icephobic coatings is not simple because several thermodynamic conditions occur during the flight (i.e. pressure and temperature change with the altitude and consequently the clouds and the supercooled water droplets change) and in addition the airflow around the aeronautical components involves the dynamic effect of impingement of the droplets on the surfaces (i.e. not only the static pressure will be present but also dynamic pressure that changes the behaviour of the droplets on the surface).[11–14] The icephobic coating could be obtained starting from super-hydrophobic behaviour; however, the icephobic coating must overcome several severe boundary conditions, some of which are reported in Fig. 1 and summarised.

Roughness rigidity

Pressure on micro and/or nanoroughness of the coating is due to the impinging of supercooled water droplets. Droplet impact can cause water droplet pressures as high as 10^5 Pa and destroy or wear the coating during the lifetime. In addition, it is important to have a behaviour of water droplet according to the Cassie–Baxter state. The maintenance of the Cassie–Baxter state requires Euler stability of the roughness, which means that the surface asperities must have resistance to buckling when water droplets impact on them.

Effect of droplet size

In the clouds there are small droplets of the order of 5–20 μm of diameter and also large droplets of the order to 300–600 μm of diameter. The impact on the component happens in a random way.

It was observed that changing the droplet size, a transition from Cassie–Baxter to the Wenzel regime can occur and vice versa. It is evident that this transition takes place as a function of the geometrical dimension of the roughness of surface. Therefore, it should be necessary to identify the range of roughness dimension where the transition does not occur.

Pressure and droplet velocity

In order to design super-hydrophobic/icephobic surfaces, the effect of impinging water droplets has to be considered. These water droplets can travel at high velocities

CIRA – Italian Aerospace Research Centre, Via Maiorise 1, 81043 Capua, Italy

*Corresponding author, email l.mazzola@cira.it

Published by Maney on behalf of the Institute
Received 16 September 2015; accepted 11 November 2015
DOI 10.1080/02670844.2015.1121319

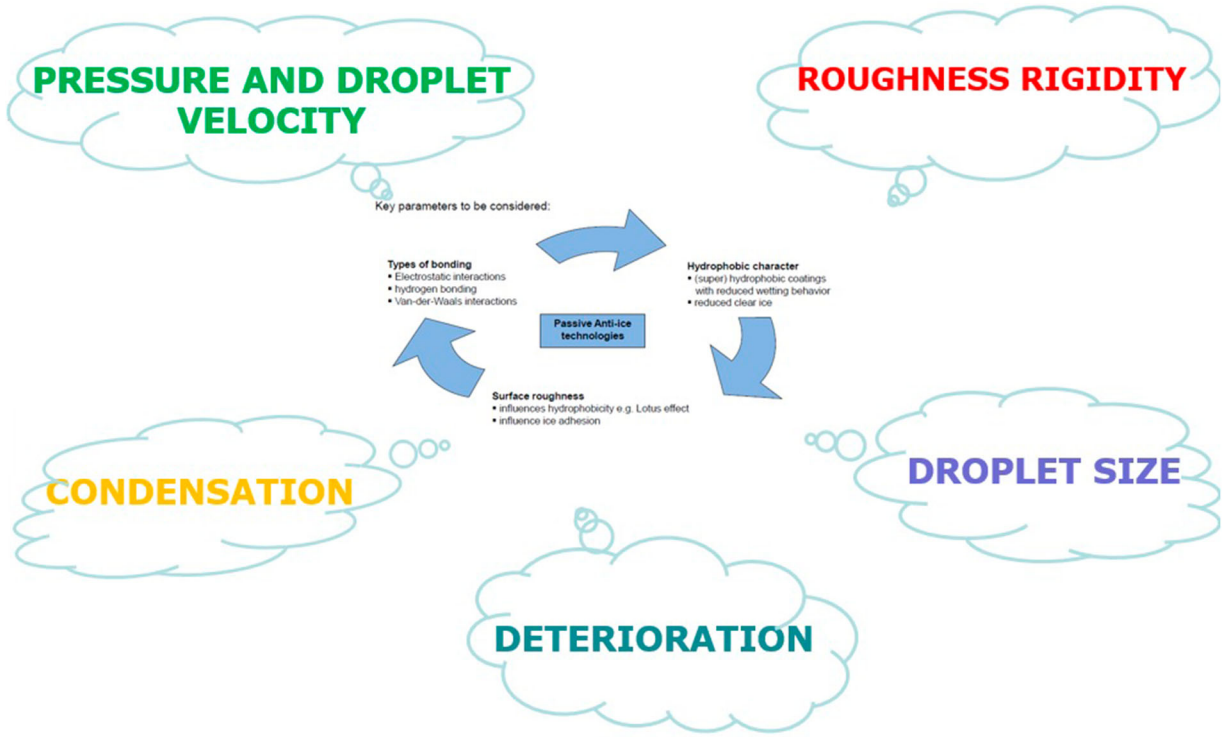

1 Sketch that shows the complexity of phenomena that must be taken into account during the design of icephobic surfaces

and exert high pressures onto surfaces upon impact. In order to ensure the functionality of super-hydrophobic surfaces in specific applications, it is crucial to prevent water infiltration into textures. At the instant of impact a shock wave is set up in the droplet, giving rise to the so-called water hammer pressure:

$$P_{WH} = 0.2 \cdot \rho \cdot C \cdot V \tag{1}$$

where ρ is the density of the liquid; C is the speed of sound in the liquid and V is the droplet velocity. After the instant of impact the wetting pressures drop is given to the familiar Bernoulli pressure:

$$P_B = \frac{\rho \cdot V^2}{2} \tag{2}$$

The water hammer pressure is significantly higher than the Bernoulli pressure. For example for a droplet impinging on a surface at 3 m s^{-1}, the water hammer pressure is 0.9 MPa and Bernoulli pressure is 4.5 kPa. In order to facilitate the complete droplet recoil and then prevent droplet infiltration, the super-hydrophobic surface should be designed so that the capillary pressure P_C exceeds both the water hammer and Bernoulli pressures $((P_B < P_{WH} < P_C))$ to have the complete recoil.

Condensation phenomena

The anti-icing properties significantly deteriorate in humid conditions, due to water condensation both on top and between the surface asperities. When microscopic water droplets are entrapped in the features of the surface during condensation, we get a composite surface consisting of solid and water instead of solid and air. The Cassie–Baxter regime does not happen and the actual contact angle obtained depends on the fraction of the surface area that is filled with water.

Deterioration of the surface

The anti-ice performances of various super-hydrophobic surfaces can change during the life time.

In fact the icephobic properties deteriorates with increasing icing/deicing cycles, a phenomenon attributed to damage on the surface structures. The top of the surface asperities have a tendency to indent into the water droplet, and when the droplet freezes and expands, mechanical tension is created that leads to damage and breakage. When the next icing event starts, the water droplet will therefore sit deeper on the surface, and the solid-ice interface area will increase, thereby increasing the ice adhesion.

To avoid this phenomenon a rounded shape roughness is needed to obtain.

Considering all of these environmental factors, it is evident that the airflow plays a key role on the impact of water droplets on components. In fact, the harsh point is represented from the stagnation point. The stagnation point represents the small region in which the supercooled liquid droplet impacts the component (such as the wings) and the dynamic pressure is equal to zero. As a consequence, after the water hammer pressure, the supercooled water droplet is undergone only to the static pressure of flight altitude. This part of the component represents the most exposed and the most subjected to ice accretion. On the contrary, in the other part of the component, the airflow is present and consequently dynamic and static pressures occur. It is necessary to consider that the dynamics of interactions between the water droplets and surface happen in a few milliseconds. The crucial time is the impact and the subsequent instant time. In fact once the droplet starts to roll on the surface component, the adhesion of supercooled water droplet is avoided.

The main theoretical prerequisites for the design of icephobic surfaces are usually considered in the context of

surface phenomena that occur at the liquid–solid interface, because ice deposits on the surfaces of the components.[15,16] When water is deposited on the surface in the solid–liquid–gas ternary system, the adhesion between the liquid and solid (upon transformation of water from the liquid state into the solid state) is provided as a result of different intermolecular (van der Waals or chemical) interaction forces.[17] According to the thermodynamic concept of adhesion, the adhesive bonding between the ice and the surface is predominantly governed by the ratio between the surface tensions of the phases (water and substrate material) and wetting.[18–23] In this case, it is assumed that solidification of water does not lead to a considerable change in the adhesion.[24]

It is clear that the characterisation on a lab scale of the icephobic surfaces thorough contact angle measurement techniques[25,26] represents a conservative method to characterise as first step the icephobic behaviour of the surfaces. For this reason it is necessary to replicate as far as possible the same environmental conditions. In any cases at present, in literature,[27] these tests are carried out reducing the temperature and keeping the atmospheric pressure. This is true in case of components that work on ground where the temperatures are very low (north and south pole, Nordic countries, etc …); however, for aeronautical and aerospace components this type of approach cannot be applicable. In fact, these components work at different altitudes and consequently at different static pressure. In this work the author describes a new method to replicate, during the contact angle measurements, the thermodynamic conditions (both temperature and pressure) similar to those present at flight altitude.

Experimental methods

Materials

A pure thermoplastic polymer such as polypropylene acquired by the Goodfellow was used to calibrate the new test room for contact angle measurements. The new icephobic coating was obtained starting from the commercial coating used as livery, i.e. a matt grey livery coating. Once that the substrate was scraped with P400 sandpaper and washed, an epoxy-modified polyamide primer using volatile organic compounds exempt solvents (solvent based high solid coating) was applied in order to improve the adhesion of the topcoat, inhibit the corrosion and level the surface.

Above the primer, a water-based three-component, isocyanate cured polyurethane topcoat (in accordance to Registration, Evaluation, Authorisation and Restriction of Chemicals – REACH regulation). The formulation of the topcoat was modified in order to give further functionality, such as icephobicity without alter the aesthetical properties and the other mechanical and corrosive properties. Both coatings were deposited through spray process on substrate of carbon fibre reinforced polymer composites because this type of application is addressed mainly for unmanned air vehicle that are usually realised in composite materials.

The temperature of the substrate was 20°C during the spray process. The dimension of the spray nozzle was 1.2 mm, the temperature of air carrier of 20°C and the air-pressure of 2 bar. The drying of the coatings was realised using a drying chamber at temperature of 120°C.

New tool to characterise icephobic surfaces

In order to replicate the same thermodynamic conditions of flight, it is necessary to change both temperature and pressure. As known,[28] the surface free energy may be defined as the increase in Gibbs free energy of the whole system per unit increase in interfacial area, carried out under conditions of constant temperature and pressure, that is:

$$\gamma = \left(\frac{\Delta G}{\Delta A}\right)_{T,p} \tag{3}$$

Therefore, as described previously, as the temperature reduces, the real thermodynamic condition in flight of the chemical state of the surfaces is not replicated. Contact angle changes in case the component works at ambient pressure and temperature, at flight temperature and ambient pressure, or at temperature and pressure in flight. In order to replicate the flight conditions, a test room, to mount on a classical contact angle measurement instrument, was designed and developed at CIRA. In particular top, bottom and two lateral and parallel surfaces were realised in insulator material, such as polycarbonate of thickness of 2 mm, whereas the other two lateral and parallel surfaces were realised in aluminium Al2024-T6 of thickness of 1 mm.

It was chosen the polycarbonate because, other than thermal insulating, it is also transparent. This property is needed to capture the liquid drops applied on the surface with camera of contact angle instrument. The two lateral and parallel surfaces in aluminium were used for the heat exchange.

The top surface of the test room has a hole with an elastic membrane in order to allow the insertion of the syringe needle to deposit the liquid drop. The syringe employed was Hamilton 600 series – 5 µl. In order to reduce the temperature, dry ice pellets of 3 mm of diameter were used. As known, the dry ice (or carbon dioxide) reaches a temperature of −79°C and it could be used to reduce the temperature in the test room. For this reason, two Polystyrene containers were realised with a sliding septa (Fig. 2*a*) and applied on the two sides in contact with the aluminium faces of the test room (Fig. 2*b*).

Changing the position of septum, different heat exchange surfaces are achieved. Using this method it is possible to reach temperature of −50°C in the test room. The temperature within the test room was detected using a thermocouple K-type.

Supercooled water droplets were realised using a microliter syringe of Hamilton. Once reached the temperature and pressure in the test room, a small quantity

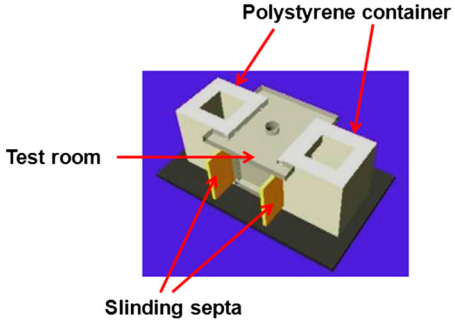

2 Rendering of the complete test room

of bi-distilled water was sucked up within the capillary of the needle. After, the needle was inserted through the elastic membrane of the test room and leaved within the room for 30 seconds, in order to reduce the temperature of the water from ambient temperature to near 0°C. After this time, the water droplet was deposited very slowly on the surface of the sample presents on the bottom of the test room. During the deposition, the water droplet had a further drastically reduction of temperature before reaching the surface of the sample, becoming supercooled. This supercooled property was simulated with a model of the heat exchange surface and phase shift of the water considering the main characteristics of the water droplet. In order to have the same flight altitude pressure, a circuit with a Venturi tube model (ZH-05-DS-06-06-06) was realised. The pneumatic circuit was composed of a main line flow starting from compressor to Venturi tube and a slipstream flow, which connected the test room and the throat of Venturi tube, as showed in the scheme reported in Fig. 3.

Using this method it was possible to reach pressure of 0.1 bar in the test room. Along with this new test room, the contact angle measurement instrument was equipped with a thermocouple display and with a pressure gauge. The complete instrument is showed in Fig. 4.

With this new tool it is possible to replicate the pressure and temperature until a flight altitude of about 16.000 m. According to the standard certification (FAR CS-25 – appendix C), the highest probability to have icing phenomena is 5.000 m, where the temperature is about −12/−15°C and pressure is about 0.5 bar. Note that the test room could be mounted on a micrometric sample-holder, which can be moved on three axes and in addition it is possible to tilt the entire test room in order to determine the advancing and receding contact angle as well as the roll-off angle.

Bi-distilled water, methylene iodide and formamide were used to determine surface free energy and its components, together with adhesion work and other performance indexes, i.e. advancing and receding contact angle, hysteresis, roll-off angle. During the test, 10 drops (with volume smaller than 3 µl) of each liquid were deposited on the sample surface. The surface free energy was calculated according to the Owens–Wendt method.[29] The Owens–Wendt approach is one of the most commonly used methods for calculating the surface free energy of the materials.[30] The principal assumption of the OW method is that the surface free energy is the sum of the two components: dispersion and polar components.[31]

The Owens–Wendt model is represented by the geometric mean relationship:

$$\frac{1}{2}(1+\cos\theta)\gamma_L = (\gamma_S^D \cdot \gamma_l^D)^{1/2} + (\gamma_S^P \cdot \gamma_l^P)^{1/2} \quad (4)$$

where θ is the contact angle between the liquid droplet and surface, γ_L is the liquid total surface tension, γ_l^D is the dispersion component of liquid surface tension and γ_l^P is the polar component of liquid surface tension.

The unknown terms in the equation (2) are γ_S^D which is the dispersion component of the solid surface free energy and γ_S^P which is the polar component of the solid surface free energy.

The value of total surface free energy of the solid is obtained using the following equation:

$$\gamma_S = \gamma_S^D + \gamma_S^P \quad (5)$$

The surface tension of liquids and its components are taken from literature.[32] However these values are referred to standard conditions of ambient temperature and pressure at sea level.

Using the Karbanda's equation, it is possible to rescale the values of surface tension from temperature point of

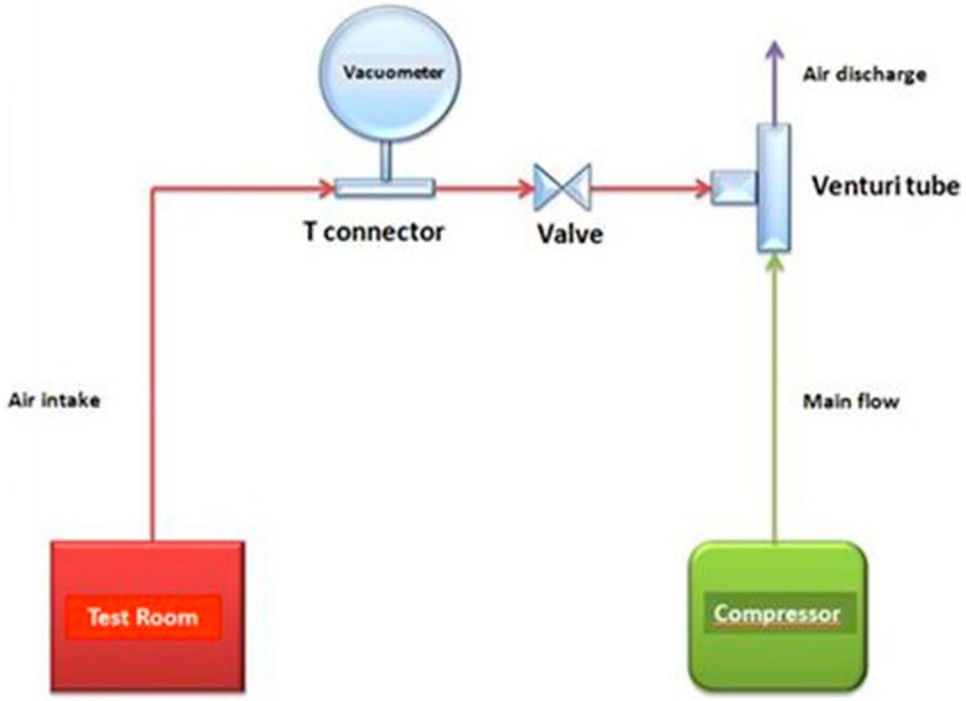

3 Scheme of pneumatic circuit

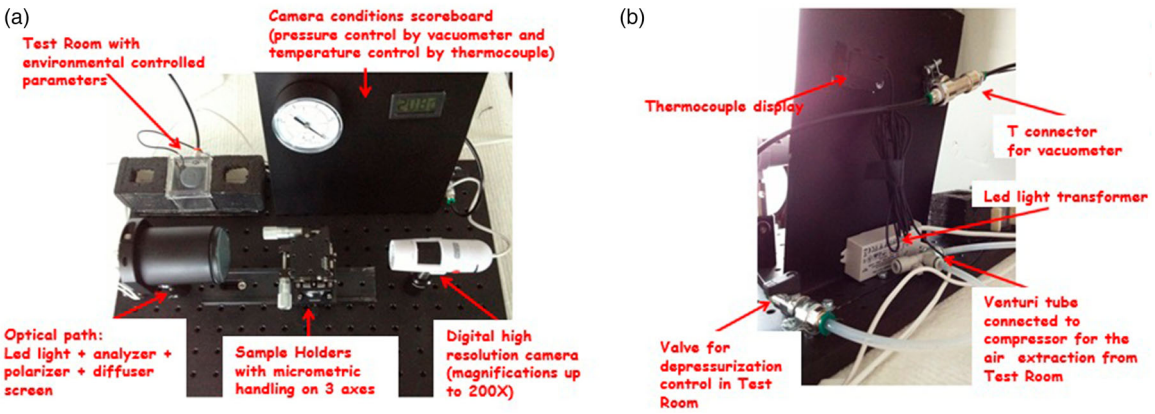

4 ***a*** **Frontal image of contact angle measurement instrument.** ***b*** **Behind image of contact angle measurement instrument**

Table 1 Values of the critical temperature of the three liquids employed

Critical temperature [°C]		
Water	Formamide	Methylene iodide
373.94	376.45	474.42

view:

$$\gamma_{T_2} = \gamma_{T_1}\left(\frac{T_c - T_2}{T_c - T_1}\right)^{1,12} \tag{6}$$

where γ_{T_1} represents the surface tension of liquid at 20°C while T_c represents the critical temperature of the liquid. The critical temperatures of the three liquids are reported in the Table 1.

Once rescaled the values from temperature point of view, it is necessary to rescale these new value for the new pressure, using the Laplace equation:

$$\gamma_{p_2} = \gamma_{p_1}\left(1 - \frac{K \cdot p_2}{200}\right) \tag{7}$$

where K is a constant value which is function of employed liquids. For the liquids employed in these experiments K equal to 2 was used. The calculation of all performance indexes of the instrument were determined using a software, designed and developed at CIRA. This software has all main models present in literature other than Owens–Wendt.

It is evident that, in the real condition, the behaviour and dynamics of the interaction between the supercooled liquid dropled and surface are more complex, because the supercooled water droplets impact with high speed on the aircraft components. The dynamics of interaction, happening in a few milliseconds, are in non-equilibrium condition and there are several phenomena that can occur, i.e. infiltration due to the water hammer pressure, instantaneous freezing or rapid rolling of the droplet.

In any case, the characterisation technique developed in this work allows to study the icephobic surface in static conditions. This represents the worst condition since the supercooled water droplet has a long time to reach the equilibrium state and to freeze on the surface.

Morphological and mechanical characterisation

A ESEM-FEG (FEI producers) was used to realised the morphological characterisation. Samples were previously metallised and subsequently analysed by ESEM. An high tension of 30 kV was used.

In order to determine the mechanical properties, such as hardness and elastic modulus, a nanoidenter NHT, CSM Instruments, Peseux, CH was used, according to the standard test ISO 14577. The tip employed was a Berkovich. It was preliminarily calibrated on silicon. All tests were performed in load control, with maximum load of 3 mN which is equivalent to the 800 nm of penetration depth. The load speed was 4.50 mN min^{-1} and holding time at maximum load of 30 seconds. On each sample were performed 40 indentations.

In order to evaluate the adhesion of the new icephobic formulation to the substrate, two different standard test methods were performed, i.e. cutting and tape test (ASTM D3359 method B and DIN standard n. 53151), which could be defined as a qualitative method to determine first of all the damage of the carving and subsequently to evaluate the number of the small squares detached from the substrate.

Further pull-off test (ASTM D4541) was performed. It is a quantitative method to evaluate the normal force necessary to remove or separate the coating from the substrate. Tests were performed with the tensile tester Instron 4505.

Resistance to aircraft hydraulic fluids

The resistance of hydraulic fluids was performed using Skydrol LD-4 for 30 days at 25°C according to the standard tests, i.e. MIL-PRF-83282, STANAG 4360. Skydrol is the most advanced aviation hydraulic fluid supported by recognised experts in phosphate-ester fluid technology. The aim of this standard test is to evaluate if at the end of the experiment delamination, blistering or lack of adhesion occurred.

Results and discussion

In order to calibrate and test the new test room, experimental tests were performed on standard material such as polypropylene; it is known that its wettability is about 90–110° and surface free energy is about 30–35 mJ m^{-2} in standard condition (temperature of 20°C and pressure of 1 bar). These two values

were taken as reference data to compare with those obtained in 'flight' conditions. Tests on polypropylene with new test room were realised simulating the highest risk of icing that occurs at 5.000 m. At this altitude the temperature reaches to −15°C and pressure arrives to 0.5 bar. Results regarding the wettability are reported in Figs. 5 and 6.

The blue dots in Fig. 5 represent the value at ambient pressure (1 bar); it is evident that the contact angle decreases, reducing the temperature. This means that the surface becomes more hydrophilic than in the ambient temperature. The red dots represent the value at pressure of 0.5 bar, reducing the temperature until to −15°C. It is evident that the trend is the same of the experimental data at ambient pressure (blue dots), however they are shifted downward. This has a consequence that hydrophilicity is improved.

In Fig. 6, the shapes of the drops and the contact angle values of the experimental points from standard condition of pressure and temperature (point A) to the flight conditions at temperature of −15°C and pressure of 0.5 bar (point E) are reported. Comparing the extreme points A and E, the surface showed an improvement of wettability of 35%. Analysing these results, it emerges that it is important to take into account the thermodynamic properties of the environment in which the surface works. In fact the risk might be to realise a surface that could seem hydrophobic or super-hydrophobic, but in the real working condition it appears partially hydrophilic. A further confirmation of these statements is described in Fig. 7, where the trend of surface free energy is showed.

The trend is in the opposite compared to the wettability; in fact, the surface free energy increases as the temperature decreases, and reducing the pressure the trend is the same but shifted upward. This means that, compared to the standard flight conditions, the surface has the highest surface free energy. So the surface has potentially more energy to create adhesion. Comparing the extreme points A and E, the surface showed an improvement of surface free energy of 59% (from 34.96 to 84.97 mJ m^{-2}). This statement is corroborated, analysing the graph of work of adhesion between water and surface (Fig. 8).

In fact the work of adhesion between water and the surface of polypropylene increases, as the temperature and pressure reduce. Comparing the extreme points A and E the surface showed an improvement of surface free energy of 42% (from 60.33 to 102.64 mJ m^{-2}).

From a physical point of view this means that an improvement of the chemical bonds between water and surface is obtained.

Tests with the new tool were performed both on a classical livery coating and on the new icephobic formulation. In particular 10 droplets of each liquid: bidistilled water, diiodomethane and formamide were deposited on the surfaces in order to determine surface free energy and its components (polar and dispersion components). Tests were performed in standard conditions, i.e. ambient temperature and pressure at sea level, and in simulated flight conditions, i.e. temperature of −12°C and pressure of 0.5 bar. As reported in Fig. 9, the great difference between the water contact angle of the commercial coating and the new icephobic formulation is evident.

From Fig. 9*a* and *b*, it is evident that the two samples have the same aesthetical aspect. No differences in terms of colour, gloss, brilliance are evident. The two samples seem the same, but, as showed in Fig. 10*c* and *d*, the behaviour of the freezed water droplet on the surface is completely different. The commercial coating is hydrophilic, whereas the new formulation has super-hydrophobic/icephobic behaviour. It is necessary to highlight that this static condition represents the harsh condition in which the coating will work. In fact, as described previously, the coating is under airflow. Therefore the water droplet does not remain on the surface but it starts to roll away. It is evident that in case of hydrophilic coating, as reported in Fig. 9*a* and *c*, this behaviour does not happen, at most it tends to slide away.

In any case, in Fig. 9*c* and *d* the contact angle measurements of the supercooled water droplets applied on both samples are reported. The commercial coating has a water contact angle of about 48°, whereas the new icephobic coating has a water contact angle of about 160°. The improvement of water contact angle was higher than 70%.

Realising also the contact angle measurements with other two liquids (formamide and diiodomethane), it was possible to determine the surface free energy and other chemical and physical performance indexes.

As showed in Fig. 10, a drastic reduction of these performance indexes is evident; in fact the surface free energy decrease of the 85%, whereas the dispersion component of the 77% and polar component of 99%. Note that the polar component mainly influences the adhesion between water droplet and the surface, therefore the drastic reduction of

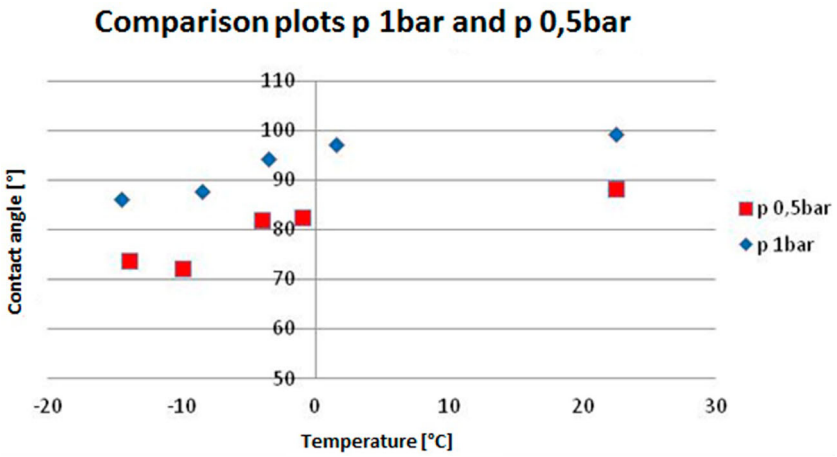

5 Trend of wettability at five different temperature and two values of pressure

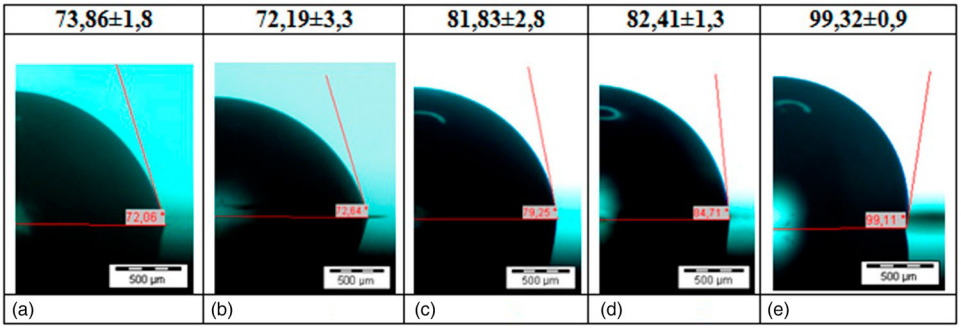

6 Variation of the behaviour of the water droplet on a surface changing pressure and temperature

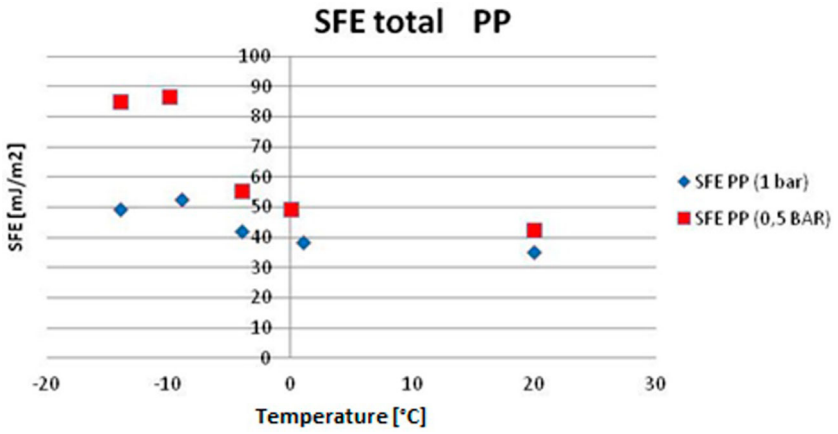

7 Trend of the surface free energy changing temperature and pressure

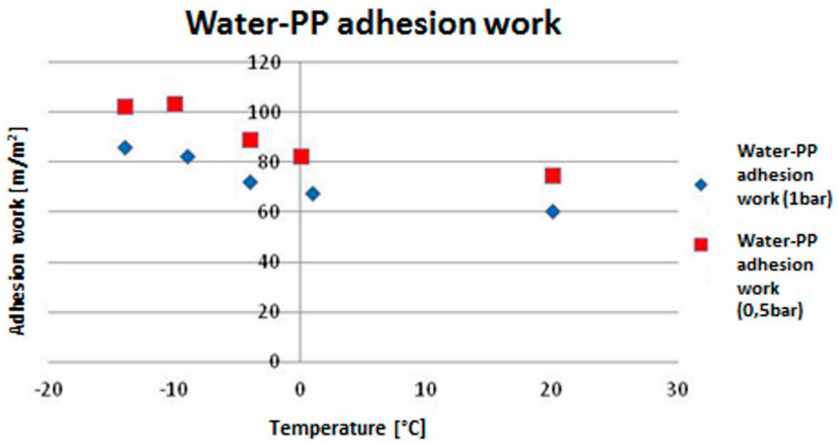

8 Work of adhesion between water and polypropylene surface

this component allows to estimate the reduction of the adhesion of water.

This last statement is also confirmed by the experimental values of work of adhesion. In fact author calculated the work of adhesion of the classical commercial coating and the new icephobic formulation. The reduction of the 92% is evident from Fig. 11.

The different behaviour of the two coatings is due not only to the different chemical composition of the surface but also to the different morphology of the two coatings. In fact, as showed in Fig. 12*a*–*c* at three different magnifications, it is evident that the classical commercial coating shows a smooth surface.

Whereas the new anti-ice formulation shows a surface rougher than commercial one (as showed in Fig. 12*d*). In particular in Fig. 12*e* several micro-features are showed; in addition, improving the magnification on each micro-feature, a nanostructure is evident. A spherical shape roughness is described in Fig. 12*e*.

Therefore, it is possible to conclude that a hierarchical structure is obtained, similar to those present in nature such as lotus leaf. This hierarchical structure allows the coating to have super-hydrophobic properties; such roughness promotes the entrapment of air or vapour within the micro and nanofeatures and the wetting of such surface is predicted by Cassie–Baxter wetting model.

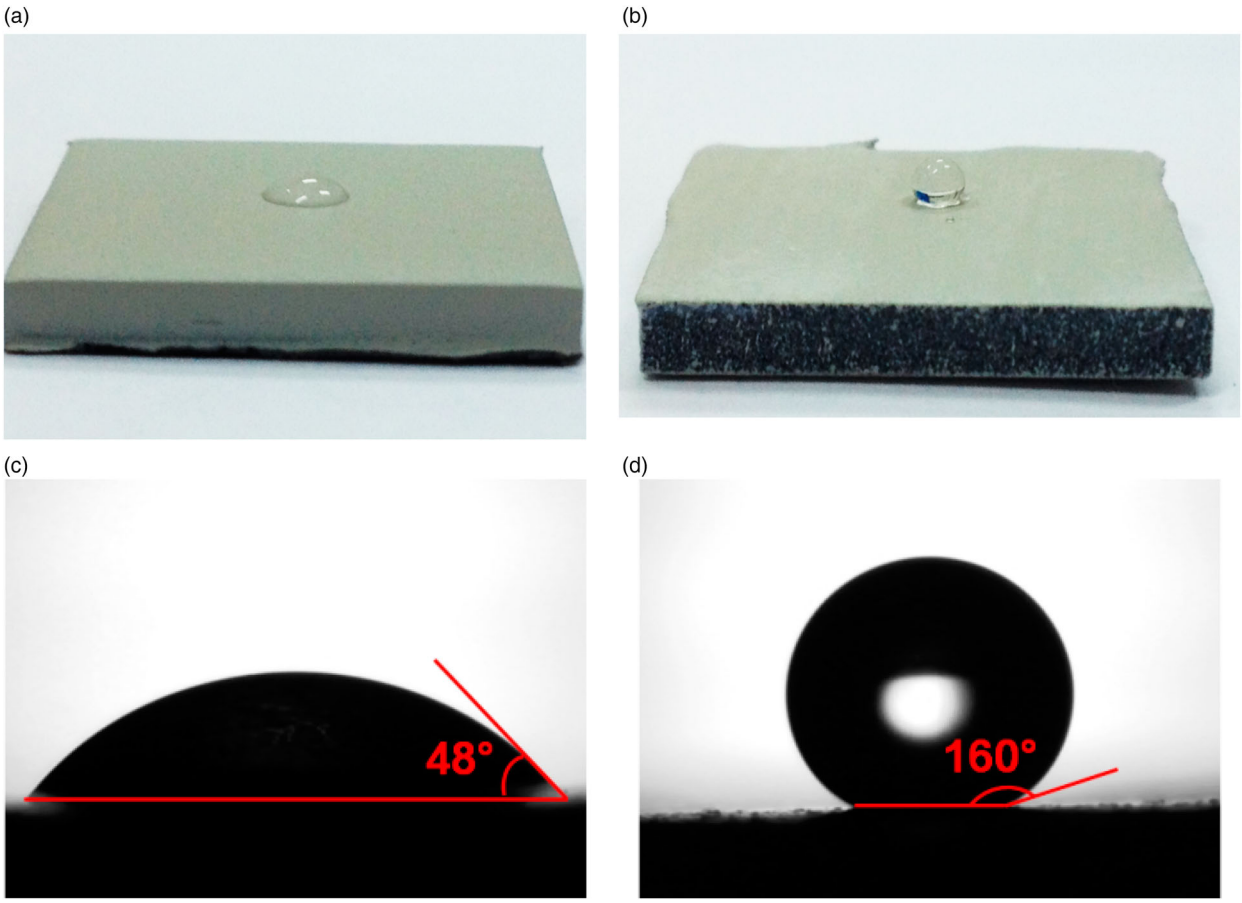

9 ***a*** **Image of sample with commercial coating. It is evident the freezed water droplet on the surface which spreads on the surface.** ***b*** **Image of sample with new icephobic coating. It is evident the freezed water droplet on the surface which assumes a spherical shape on the surface. c Micrography obtained during the contact angle measurements in which is evident that the contact angle is under 50° for the commercial coating.** ***d*** **Micrography obtained during the contact angle measurements in which is evident that the contact angle is about 160° for the new icephobic coating**

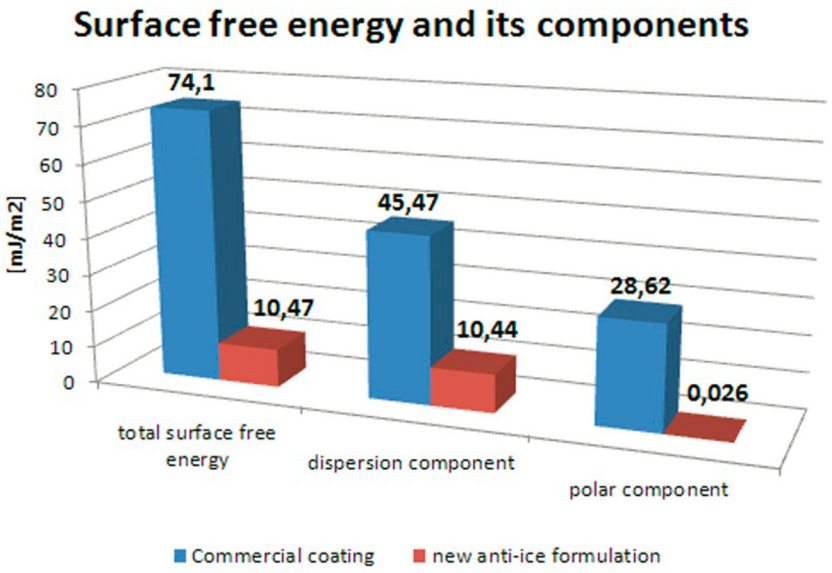

10 Comparison of the experimental data of the surface free energy and its components both for classical formulation and for the new anti-ice formulation

In particular, the droplet touches only the crests of the roughness and air pocket remains entrapped between the droplet and the surface.

Even if the morphological aspect is extremely important to have super-hydrophobicity and icephobicity, it is also important to preserve it for the entire cycle of flight

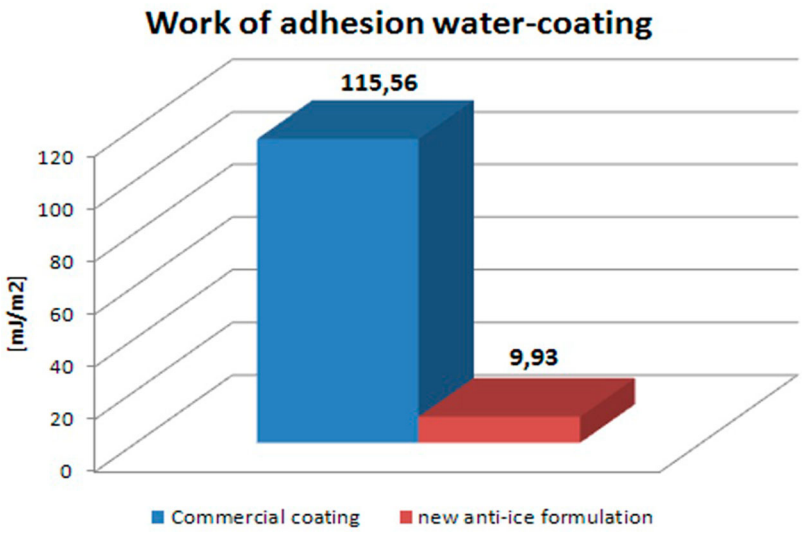

11 Comparison of the work of adhesion between the classical commercial coating and the new formulation with anti-ice properties

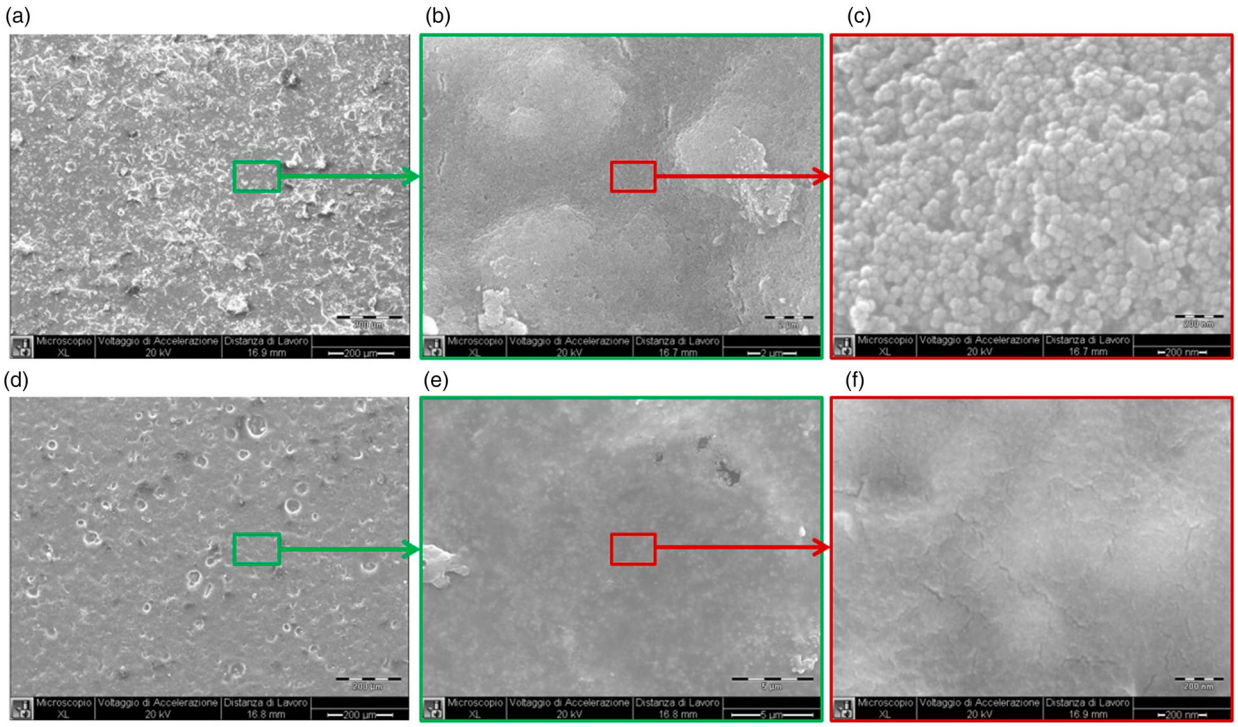

12 *a* Reference sample surface, magnification 300×. *b* Reference sample surface, magnification 10 000×. *c* Reference sample surface, magnification 150 000×. *d* Icephobic sample surface, magnification 300×. *e* Icephobic sample surface, magnification 10 000×. *f* Icephobic sample surface, magnification 150 000×. It is evident the hierarchical structure of the icephobic coating. A micro-features are well visible in the *d* and *e* and in the *f* the nanofeatures are evident

from one maintenance and other of the aircraft. For this reason, it is important to evaluate the mechanical properties of the new coating. In fact, as described previously, the keeping of the icephobic properties of the new coating is correlated with the mechanical properties, such as hardness and elastic modulus. In fact, it is necessary to point out that this functionalised coating undergoes severe operating conditions during the flight. In particular, the surface is subjected to the impact of sand, dusts, insects, rain, which can alter its original morphology; as a consequence, the icephobic property can be lost.

The main mechanical properties are reported in Table 2. Hardness and elastic modulus of the new icephobic coating are the same of the commercial coating used as reference.

Results of cutting and tape tests are reported in Fig. 13, where the same behaviour of the two coatings is evident. In fact, according to the standard classification of the

Table 2 Nanoindentation results regarding the commercial coating and the new formulation

	Commercial coating	New anti-ice formulation
HIT [MPa]	157 ± 16	141 ± 9
$HV_{0.003N}$	14.57 ± 1.41	13.06 ± 0.85
EIT [GPa]	4.60 ± 0.63	4.84 ± 0.28

percentage of removed area, the two coatings show the same classification, 5B. However, from Fig. 13*a*, it is evident that the new icephobic formulation seems less damaged than the other. The scratches seem to be shallower than those of the commercial coating.

This statement was confirmed by the results obtained with pull-off test (Fig. 13). In fact, the critical load of the commercial coating was of 0.607 ± 0.068 kN whereas the new icephobic formulation has a critical load of 0.756 ± 0.012 kN.

The results of pull-off tests demonstrated the higher adhesion to the substrate of the new icephobic coating compared to the commercial one. In fact, the improvement of adhesion between coating and substrate was higher than 24% for the new formulation (Fig. 14).

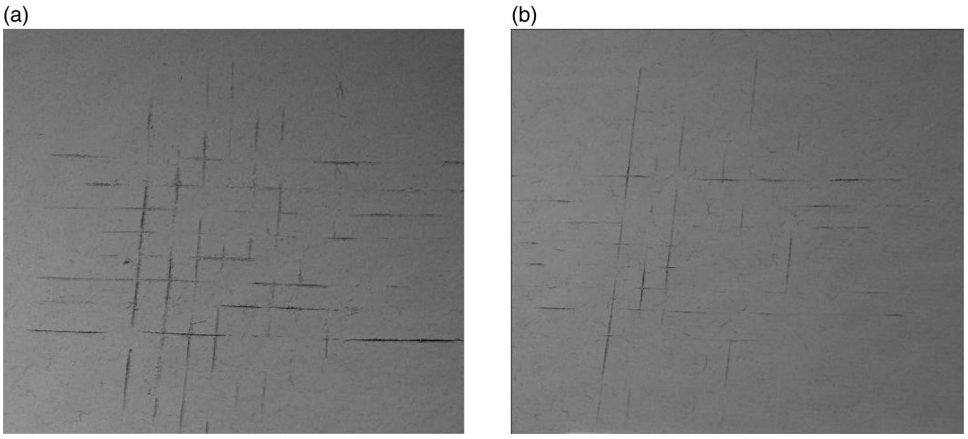

13 ***a*** **Cutting and tape test of the commercial coating. The classification of the adhesion is 5B according to the standard classification.** ***b*** **Cutting and tape test of the new anti-ice formulation. The classification of the adhesion is 5B according to the standard classification**

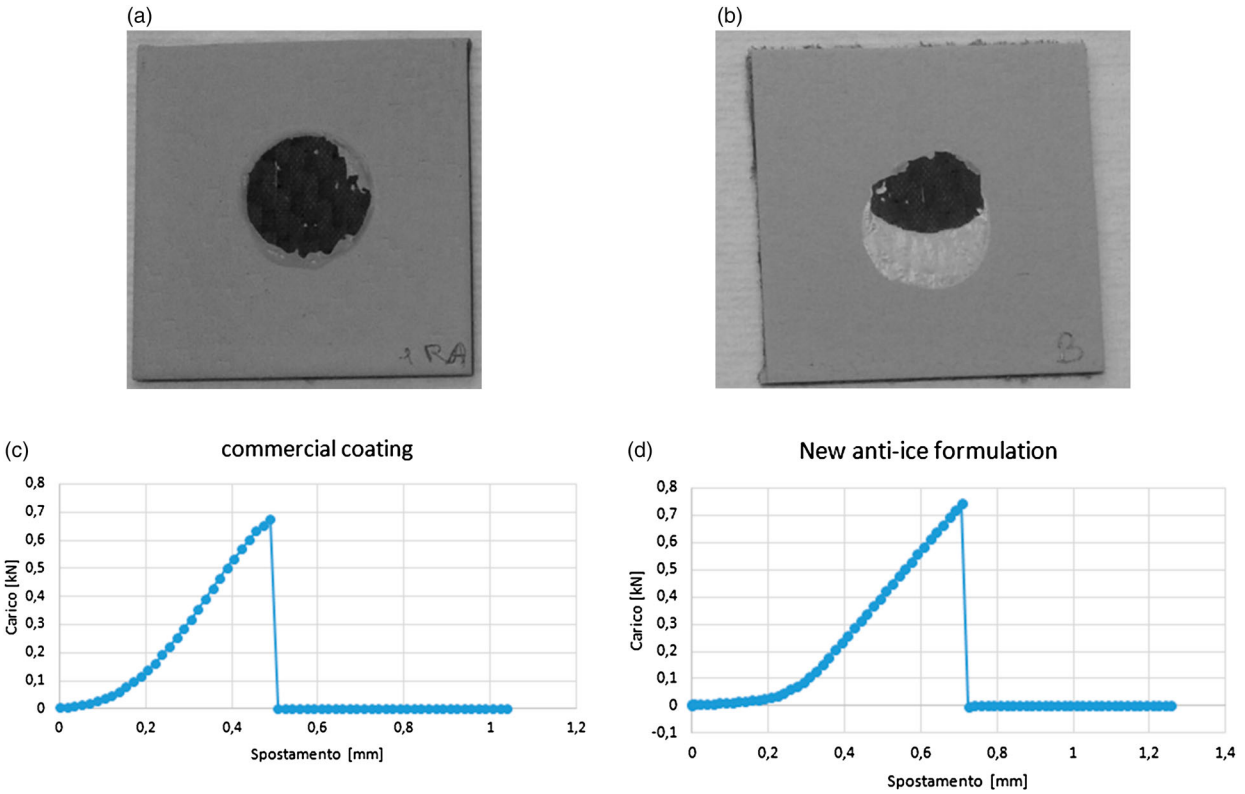

14 ***a*** **Pull-off test of the commercial coating. It is evident the adhesive fracture between coating and substrate.** ***b*** **Pull-off test of the commercial coating. It is evident the adhesive fracture between coating and substrate and cohesive fracture within the coating.** ***c*** **Experimental data of the critical load [kN] and displacement [mm] for the commercial coating.** ***d*** **Experimental data of the critical load [kN] and displacement [mm] for the new anti-ice formulation**

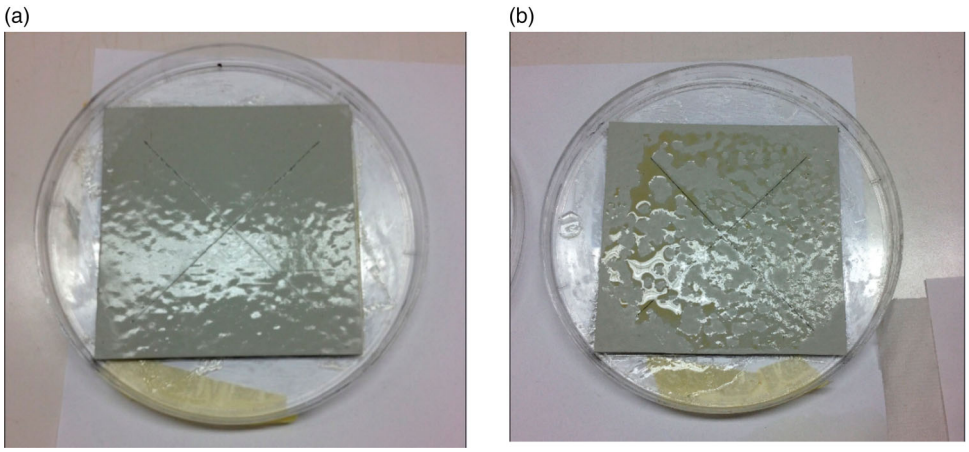

15 ***a*** **Behaviour of the commercial coating after 30 days.** ***b*** **Behaviour of the new anti-ice formulation after 30 days. It is evident the different behaviour of the liquid droplet respect to the commercial coating**

Finally, resistance to hydraulic fluids was performed. In particular according to the standard test, droplets of Skydrol were applied on the two surfaces (commercial coating and new icephobic formulation) for 1 month.

As reported in Fig. 15, the new icephobic formulation as well as the commercial coating did not show blistering, delamination, colour changes. In addition, it is interesting to highlight that the Skydrol applied on commercial coating creates a thin and uniform film on the coating. On the contrary, the new icephobic formulation showed a different behaviour; in fact the Skydrol did not create a film but remained in macro-droplets on the surface. The different behaviour is due to the super-hydrophobic property of the new formulation. This represents a further advantage because the super-hydrophobicity preserves the surface of the new coating.

Conclusions

In this work a multifunctional aeronautical coating with aesthetic and icephobic properties was designed, developed and characterised.

To evaluate the icephobicity, a new tool to apply on contact angle measurement instruments was designed and developed. The new tool is very useful to modify the thermodynamic conditions of pressure and temperature. It is possible to replicate the values present at flight altitude. The more realistic environment simulation allows to have a more truthful behaviour of the coating.

Using this method, the super-hydrophobicity and icephobicity of the new coating, compared to the commercial one, was demonstrated.

The surface free energy is decreased of 85%, the dispersion component of 77% whereas the polar component is not present. These values are also corroborated by the work of adhesion between supercooled water droplet and surface that has a drastic reduction of 91%.

These results are due to the different surface chemistry of the coatings but also to the different morphology (the icephobic coating shows a hierarchical structure). It is interesting to highlight that even if the morphology is different, the macroscopic exterior aspect in terms of aesthetical properties is the same (colour, gloss and brilliance) of that of the commercial one.

The durability of the new coating was corroborated by nanoindentation tests, adhesion tests and corrosive tests. In particular hardness and elastic modulus are the same whereas the adhesion of the icephobic coating to the substrate was 24% higher than the commercial one. The new icephobic coating has the same resistance to hydraulic fluids than the commercial coating.

This new icephobic coating represents a great success from an industrial point of view. In fact, the great aeronautical end-users confirmed and validated the applicability of this coating on industrial scale. At this time the replication of the spray process of this new formulation on industrial scale was validated. Future activities are intended to verify that this new coating overcomes all aeronautical standard tests for a future certification.

Acknowledgements

Author would like to thank Prof. Luca Lusvarghi, Dr. Giovanni Bolelli, Dr. Paolo Sassatelli for the nanoindentation tests that were performed at the Engineering Department of University of Modena e Reggio Emilia.

References

1. F. Wang, C. Li, Y. Lv and Y. Du: 'A facile super hydrophobic surface for mitigating ice accretion', IEEE 9th Int. Conf. on 'Properties and applications of dielectric materials', Harbin, 19–23 July 2009, IEEE, 150–153.
2. L. B. Boinovich and A. M. Emelyanenko: 'Anti-icing potential of super hydrophobic coatings', *Mendeleev Commun.*, 2013, **23**, 3–10.
3. L. Boinovich, A. M. Emelyanenko, V. V. Korolev and A. S. Pashinin: 'Effect of wettability on sessile drop freezing: when super hydrophobicivity stimulates an extreme freezing delay', *Am. Chem. Soc.*, 2014, **30**, 1659–1668.
4. L. Makkonen: 'Ice adhesion-theory, measurements and countermeasures', *J. Adhes. Sci. Technol.*, 2013, **26**, 413–445.
5. M. Susoff, K. Siegmann, C. Pfaffenroth and M. Hirayama: 'Evaluation of icephobic coatings-screening of different coatings and influence of roughness', *Appl. Surf. Sci.*, 2013, **282**, 870–879.
6. G. Momen and M. Farzaneh: 'Facile approach in the development of icephobic hierarchically textured coatings as corrosion barrier', *Appl. Surf. Sci.*, 2014, **299**, 41–46.
7. T. Strobl, S. Storm, M. Kolb, J. Haang and M. Hornung: 'Development of a hybrid ice protection system based on nanostructured hydrophobic surfaces', Proc. 29th Congress of the International Council of the Aeronautical Science, St. Petersburg, Russia, September 2014.
8. A. Lazauskas, A. Guobiene, I. Prosycevas, V. Baltrusaitis, V. Grigaliunas, P. Narmontas and J. Baltrusaitis: 'Water droplet

behavior on super hydrophobic SiO_2 nanocomposite films during icing/deicing cycles', *Mater. Charact.*, 2013, **82**, 9–16.
9. L. Zhu, J. Xue, Y. Wang, Q. Chen, J. Ding and Q. Wang: 'Ice-phobic coatings based on silicon-oil-infused polydimethylsiloxane', *Appl. Mater. Interface*, 2013, **5**, (10), 4053–4062.
10. D. Attinger, C. Frankiewicz, A. R. Betz, T. M. Schutzius, R. Ganguly, A. Das, C. Kim and C. M. Megaridis: 'Surface engineering for phase change heat transfer: a review', *MRS Energy Sust. Mater. Res. Soc.*, 2014, **1**, 1–40.
11. C. Laforte, C. Blackburn and J. Perron: 'A review of icephobic coating performances over the last decades', *SAE Tech. Pap.*, 2015, **01**, 2149.
12. H. Saito, K. Takai and G. Yamauchi: 'A study on ice adhesiveness to water-repellent coating', *Mater. Sci. Res. Int.*, 1997, **3**, (3), 185–189.
13. S. A. Kulinich and M. Farzaneh: 'Ice adhesion on super-hydrophobic surfaces', *Appl. Surf. Sci.*, 2009, **255**, (18), 8153–8157.
14. S. A. Kulimich, S. Farhadi, K. Nose and X. Du: 'Super hydrophobic surfaces: are they really ice-repellent?', *Langmuir*, 2011, **27**, (1), 25–29.
15. P. F. Riosa, H. Dodiukb, S. Kenigc, S. McCarthyd and A. Dotan: 'The effect of polymer surface on the wetting and adhesion of liquid systems', *J. Adhes. Sci. Technol.*, 2007, **21**, (3–4), 227–241.
16. K. K. Varanasi, T. Deng, J. D. Smith, M. Hsu and N. Bhate: 'Frost formation and ice adhesion on super hydrophobic surfaces', *Appl. Phys. Lett.*, 2010, **97**, (23), 234102-1–234102-3.
17. F. M. Etzler: 'Contact angle, wettability and adhesion', (ed. K. L. Mittal), Vol. 3; 2003, Utrecht, VSP.
18. K. L. Mittal: '*Advances in contact angle, wettability & adhesion*', Vol. 1; 2013, Beverly, MA, Scrivener Publishing, Willey.
19. A. J. Meuler, J. D. Smith, K. K. Varanasi, J. M. Mabry, G. H. McKinley and R. E. Cohen: 'Relationships between water wettability and ice adhesion', *ACS Appl. Mater. Interfaces*, 2010, **2**, (11), 3100–3110.
20. S. Farhadi, M. Farzaneh and S. A. Kulinich: 'Anti-icing performance of super hydrophobic surfaces', *Appl. Surf. Sci.*, 2011, **257**, (14), 6264–6269.
21. S. Jung, M. Dorrestijn, D. Raps, A. Das, C. Magaridis and D. Poulikakos: 'Are super hydrophobic surfaces best for icephobicity?', *Langmuir*, 2011, **27**, (6), 3059–3066.
22. M. F. Hassan, H. P. Lee and S. P. Lim: 'The variation of ice adhesion strength with substrate surface roughness', *Meas. Sci. Technol.*, 2010, **21**, (7), 1–9.
23. W. D. Bascom, R. L. Cottingt and C. R. Singlete: 'Ice adhesion to hydrophilic and hydrophobic surfaces', *J. Adhes.*, 1969, **1**, 246–263.
24. Y. Yuan and T. Randall Lee: 'Contact angle and wetting properties, surface science techniques', (ed. B. Holst) Springer Series in Surface Sciences 51, 2013, Bracco.
25. K. L. Mittal: 'The role of the interface in adhesion phenomena', *Polym. Eng. Sci.*, 1977, **17**, (7), 467–473.
26. K. L. Mittal: '*Contact angle, wettability and adhesion 5*', 2008, Leiden, VSP.
27. D. Gao, A. K. Jones and V. K. Sikka: 'Anti-icing super hydrophobic coatings', US Patent 0314575-A1, Dec 16, 2010.
28. R. A. L. Jones and R. W. Richards: '*Polymers at surface and interfaces*', 2006, Cambridge: Cambridge University Press.
29. D. K. Owens and R. C. Wendt: 'Estimation of the surface free energy of polymers', *J. Appl. Polym. Sci.*, 1968, **13**, 1741.
30. M. Zenkiewicz: 'Methods for the calculation of surface free energy of solids', *Pol. Test.*, 2007, **26**, 14–19.
31. A. Rudawska and E. Jacniacka: 'Analysis of determining surface free energy uncertainty with the Owens-Wendt method', *Inter. J. Adhes. Adhes.*, 2009, **29**, 451–457.
32. L. Holysz, E. Chibowski and K. Terpilowsi. 'Contact angle, wettability and adhesion', (ed. K. L. Mittal), Vol. 5, 2008, Leiden, VSP/Brill.